



FIRE IN ROAD TUNNELS. THE INFLUENCE OF THE HEAT RELEASE RATE IN THE SMOKE FLOW

Ulisses Fernandes¹, João C. Viegas¹ and Pedro J. Coelho²

1: LNEC, Laboratório Nacional de Engenharia Civil
1700-099 Lisbon, Portugal
e-mail: ufernandes@lnec.pt, jviegas@lnec.pt

2: IDMEC, Instituto de Engenharia Mecânica, Mechanical Engineering Department
Instituto Superior Técnico
Universidade de Lisboa
1049-001 Lisbon, Portugal
e-mail: pedro.coelho@tecnico.ulisboa.pt

Keywords: Tunnel fire, natural ventilation, wind, *fireFoam*, smoke propagation, CFD

Abstract *Fire accidents in road tunnels may cause a significant number of fatalities and severe damages in the tunnel structure. The tunnel European directive [1] applies to trans-European road network and requires the use of active smoke control systems for most tunnels longer than 500 m. Research has been carried out to investigate if shorter tunnels are safe when the smoke flow occurs due to buoyancy [2, 3]. The FireFoam computer code has been used to model the Memorial Tunnel fire ventilation tests [4] and validate the tunnel model. This model was used to produce a set of simulations to investigate the effect of the wind velocity and of the tunnel slope on the smoke buoyant flow.*

In a first step, the effect of the wind velocity on the smoke flow in a horizontal tunnel showed that the contamination of the lower layer (where the people egress) with smoke may start as close as 138 m from the fire source [2]. This contamination (depending on its intensity) may impair the visibility disturbing the people egress, and may cause intoxication and, eventually, death. In a second step, the effect of the slope (without wind) may increase the tendency to the lower layer contamination [3], when compared to the horizontal tunnel. Lower layer contamination may start as close as 210 m to fire source. An analytical model has been developed to predict the distance from the fire source where the lower layer contamination with smoke may occur.

In this communication, the effect of the variation of the heat release rate (HRR) both with and without wind is studied in the same tunnel model. It shows that, although the velocity due to buoyancy increases with the HRR, the location of the lower layer contamination with smoke does not vary significantly due to the increment of the flow rate. The analytical model extension to the HRR variation is also presented.

1. INTRODUCTION

Natural ventilation avoids the significant costs of mechanical ventilation in road tunnels. However, it can only be relied on as a smoke control strategy if the lower layer contamination does not happen (i.e. if the smoke remains above the occupants' height). Hence, an accurate understanding of this phenomenon under several different scenarios is important [4].

In a horizontal tunnel, the flow from a fire source is symmetrical, and the smoke forms a hot upper layer flowing from the fire plume to the tunnel portals, while a cold lower layer of outside air flows from the portals and feeds the fire plume with fresh air [3]. It is well known that the contamination of the cold lower layer with the smoke from the hot upper layer starts at some distance from the fire source, and the contaminated region increases as the smoke flows to the portals (Figure 1) [2, 3] **Erro! A origem da referência não foi encontrada. Erro! A origem da referência não foi encontrada.** The contaminated cold lower layer flow transports the smoke to the fire, and any smoke-free zone, subsisting from the beginning in the lower layer near the fire, will eventually be fully contaminated by the smoke.

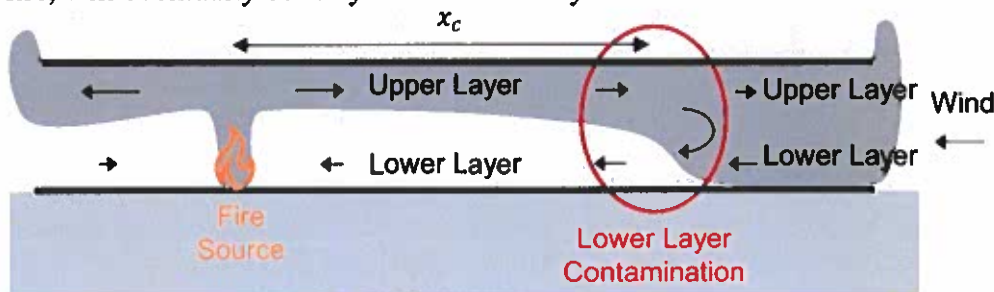


Figure 1 – Flow of smoke in a tunnel with length higher than x_c , leading to lower layer contamination [2].

The problem of the contamination of the cold layer with smoke must be analysed under three different conditions: (i) when the tunnel is completely horizontal, (ii) when the tunnel has a slope (in general, the slope does not exceed 10% and Directive 2004/54/EC [1] does not allow more than 5%) and (iii) when the wind generates a flow inside the tunnel in opposition to the smoke flow. However, most of the tunnels have a slope that, even being small, will significantly change the smoke flow and it is always necessary to consider that unfavourable wind may occur during the fire event [4]. The smoke control is used to keep the environmental conditions compatible with the occupants' safety, during the egress period of a fire, and later maintain the environmental conditions favourable for the firefighting. In this way, the smoke control may contribute to the success of the firefighting and thus prevent catastrophic consequences on the availability of infrastructure [4].

This research aims to analyse the contamination of the lower layer with smoke in horizontal tunnels with opposing wind and varying heat release rate (HRR) and this work will consider different heat release rates in the range from 6 MW to 100 MW.

2. LITERATURE REVIEW

Fires in the confined infrastructure of tunnels are critical hazards due to the potential for

fatalities and damage to the structures [5]. The tunnel European directive (Directive 2004/54/EC [1]) applies to Trans-European Road Network and states that “mechanical ventilation systems shall be installed in all tunnels longer than 1000 m with a traffic volume higher than 2000 vehicles per lane”. Therefore, there are many tunnels in Europe where the flow of smoke in the event of a fire is controlled by natural ventilation. Research has been carried out to investigate if shorter tunnels are safe when the smoke flow occurs due to buoyancy [2, 3].

Most of the studies concerned with naturally ventilated tunnels focus on horizontal tunnels, and little research has been carried out on sloped tunnels. However, most tunnels are sloped for geographical reasons, being relevant to study the smoke flow due to fires in those tunnels. In the case of fires in naturally ventilated horizontal tunnels, there are two main flows, namely, an upper layer flow that exits the tunnel and a lower layer flow that moves towards the fire. Galhardo et al. studied the effect of the wind velocity on the smoke flow in a horizontal tunnel showing that the contamination of the lower layer (where the people egress) with smoke may start as close as 138 m from the fire source [2]. The authors concluded that this contamination (depending on its intensity) may impair the visibility disturbing the people egress, and may cause intoxication and, eventually, death [2].

Ortega et al. investigated the effect of the tunnel slope on the contamination of the cold lower layer and concluded that the slope (without wind) may increase the tendency to the lower layer contamination, when compared to the horizontal tunnel, but above a certain slope, due to the stack effect, the air entering through the lower part of the tunnel changes the fire and the flow dynamics in terms of flame, temperature, velocity and smoke layer thickness [3].

One of the largest sources of experimental data from fires in a single tunnel is the Memorial Tunnel Fire Ventilation Test Program (MTFVTP) (Bechtel and Brinckerhoff, 1995 [6]). This consisted of a series of fires with varying HRR and ventilation conditions in an 853-m long tunnel with a 3.2% slope in West Virginia, USA. Natural ventilation was tested for fires with nominal HRR of 20 MW and 50 MW.

CFD simulations have become an increasingly common tool for the study of tunnel fires. Caliendo et. al [7] analysed the impact of HRR variation from 8 MW to 100 MW on the flow of smoke in a road tunnel. Kong et al. [8] investigated the effect of tunnel slope on hot gas movement and smoke distribution in a tunnel fire. They carried out a set of fire simulations, using the Fire Dynamics Simulator (FDS) software, varying the slope from 0 to 10%. More recently, Ortega et al. investigated the effect of the tunnel slope on hot gas movement and smoke distribution in a tunnel fire. They carried out a set of fire simulations, using the CFD (FireFoam) software, varying the slope from 0 to 7% [3].

In this work, CFD simulations were performed with the goal of improving the knowledge of the physical mechanisms that lead to lower layer contamination in a naturally ventilated tunnel fire. The effect of the variation of the HRR from 6 MW to 100 MW both with and without wind is studied in the same tunnel model. It shows that, although the velocity due to buoyancy increases with the HRR, the location of the lower layer contamination with smoke does not vary significantly due to the increment of the flow rate. The effect of natural wind on the flow of smoke and on the hazard to human health was analysed by comparing

predictions from simulations with varying wind velocities.

3. METHODS

3.1. CFD model

This work is based on CFD simulations using the open-source FireFOAM software package (version 1912). This code solves the Favre-filtered, three-dimensional Navier-Stokes equations using the finite volume technique and employing the pressure-implicit with splitting of operators (PISO) algorithm. Turbulence was modelled using large-eddy simulation (LES). The governing equations for mass, momentum, energy and species mass fractions are solved. The relevant physical phenomena of the flow were modelled using the Smagorinsky model for turbulence, the Eddy Dissipation Model for combustion, and the Finite Volume/Discrete Ordinates Method for radiation. These models were briefly described in Galhardo et al. [2].

3.2. CFD implementation

The CFD model was employed to perform a series of simulations of tunnel fires. The necessity of predicting the three-dimensional flow of smoke in regions spanning several hundred meters in length resulted in large computational domains. To limit the computational cost, the size of the computational domains under study was decreased by taking advantage of the symmetry of the mean flow: in all simulations, only one half of the tunnel width was simulated. On the other hand, the entire length of the tunnels under analysis was simulated, as well as two 50 m-long extensions outside the portals [4].

The CFD simulations were performed using an unstructured mesh. The control volumes of this are finest near the fire and coarser away from it, to ensure an accurate simulation of the complex flow in the vicinity of the fire source while avoiding excessively long computational times. The characteristic dimension of the control volumes, $\Delta=V^{1/3}$ (where V is the cell volume), was equal to 8 cm in the vicinity of the fire source, 16 cm in a transition region, and 32 cm elsewhere [4]. Figure 2 shows the mesh in the vertical symmetry plane for simulations shown in Table 1, where L is the tunnel length, P is the percentage of the time when the wind velocity adopted in the simulation is exceeded, V is the wind velocity, ΔP is the pressure difference generated by the wind between portals and v is the average velocity of the flow inside the tunnel due to wind velocity. The tunnel is horizontal.

The fire source was simulated as a horizontal rectangular surface and treated as a source of dodecane at boiling temperature with a vertical velocity calculated based on the desired HRR. At the walls, a no-slip condition with wall functions was used for velocity, while a zero-gradient condition was used for mass fractions of chemical species. An energy balance boundary condition was implemented to calculate the wall surface temperature. The gradient of all variables was set to 0 at the symmetry planes.

At the open borders, the ambient values of temperature and species mass fractions were prescribed for the case of inflow and a zero gradient boundary condition was set for the case of outflow. The variable p' , which represents the pressure deviation from the hydrostatic field, had different values for outflow and inflow, according to the following equation:

$$p' = \begin{cases} p_0 - \frac{1}{2}\rho|\mathbf{u}|^2 & \text{flow into the domain} \\ p_0 & \text{flow out of the domain} \end{cases} \quad (1)$$

where ρ , \mathbf{u} and p_0 stand for the density, velocity vector and free stream pressure, respectively. The values of p_0 at the two ends of the computational domain can be adjusted to create a pressure difference between the two portals, which simulates longitudinal wind flow. In the simulations the wind is acting from right to left.

L [m]	P [%]	V [m/s]	ΔP [Pa]	v [m/s]	HRR _{nominal} [MW]
600	20	3.13	3.61	1.19	100
600	35	2.04	1.54	0.771	6
600	35	2.04	1.54	0.771	15
600	35	2.04	1.54	0.771	50
600	35	2.04	1.54	0.771	70
600	35	2.04	1.54	0.771	100
600	100	0	0	0	6
600	100	0	0	0	50
600	100	0	0	0	100

Table 1 - Simulation parameters

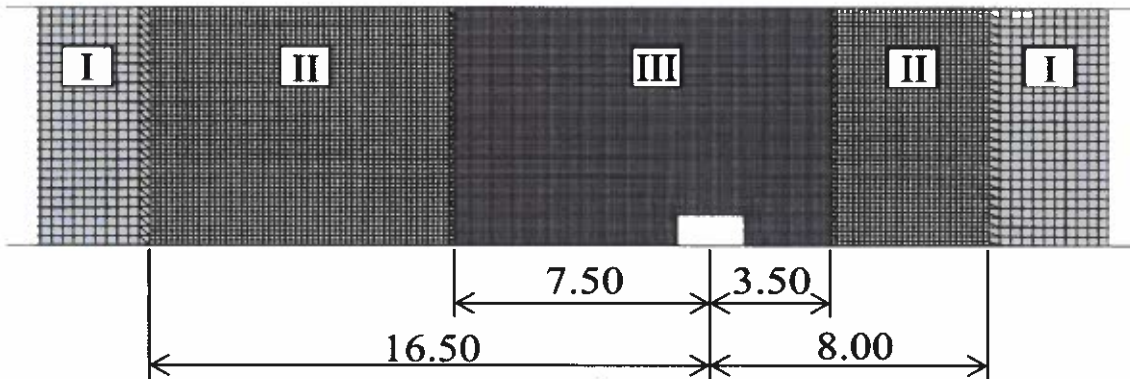


Figure 2 – Mesh refinement near the fire source in simulations (dimensions in m)

3.3. CFD validation

The CFD model was validated by simulating the test 502 of the Memorial Tunnel Fire Ventilation Test Program (MTFVTP); details about the tunnel geometry and the test conditions may be found in Bechtel and Brinckerhoff [6]. The tests were carried out for a naturally ventilated tunnel. The fire source was a pool fire of Fuel Oil No.2 (modelled as dodecane). The nominal heat release rate (HRR_{nominal}) was 50 MW.

Figure 2 shows the validation for the HRR of 50 MW (temperatures in Fahrenheit). The

predicted temperature field is slightly colder in comparison with the experimental data [4].

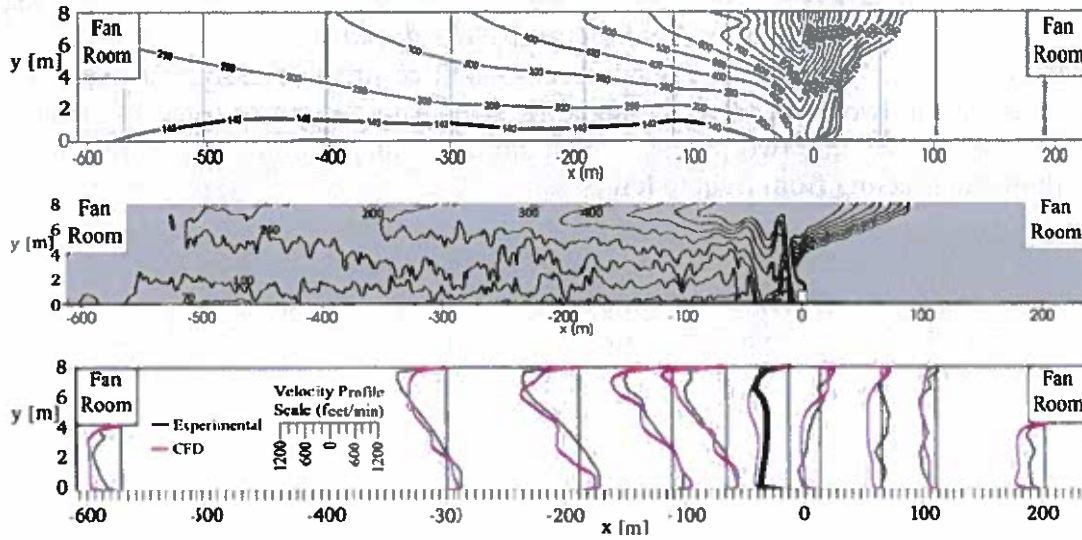


Figure 2 – Comparison of the temperature and velocity measurements obtained for the MTFVTP test 502 with the CFD predictions (natural ventilation, $HRR_{nominal} = 50$ MW, $t = 10$ min)

4. SIMULATION RESULTS

The purpose of this work is to better understand the processes of contamination of the tunnel lower cold layer with the smoke coming from the hot upper layer, considering different conditions of HRR and velocity of the external wind.

After the validation, several cases were studied to assess the effect of the HRR in horizontal naturally ventilated fire tunnels and its impact on the distance from the fire source to the location where the contamination of the lower layer with smoke starts. CFD simulations for HRR ranging from 6 MW to 100 MW were carried out, with wind effect and without wind action and considering only natural ventilation.

Figure 3 presents the longitudinal profiles of the average temperature at the cross section of the upper layer (calculated according to the equation 2, where T_{∞} is the ambient temperature, ρ is the density, u is the velocity, $\overline{C_p}$ is the specific heat at constant pressure, \dot{m} is the mass flow rate and A is the cross section area) and Richardson Number (Ri) along the horizontal tunnel (from fire to the portal) for simulations with varying HRR ($v=0.77$ m/s and $P=35\%$). The Ri is defined in the equation 3, where h_u represents the upper layer thickness and $\Delta\rho$ the difference between layer densities.

$$\bar{T} = T_{\infty} + \frac{\int_{UL} \rho u \overline{C_p} (T - T_{\infty}) dA}{\dot{m} \overline{C_p}} \quad (2)$$

$$Ri = \frac{\Delta\rho g h_u}{\rho (|u_u| + |u_l|)^2} \quad (3)$$

Figure 4 presents the profiles of the same quantities for HRR=100 MW with wind ($v=1.19$ m/s and $P=20\%$) and Figure 5 shows the profiles for varying HRR without wind ($v=0$ m/s and $P=100\%$).

For the horizontal tunnel, the temperature decays exponentially from the fire source to the exit portal (Figures 3, 4 and 5).

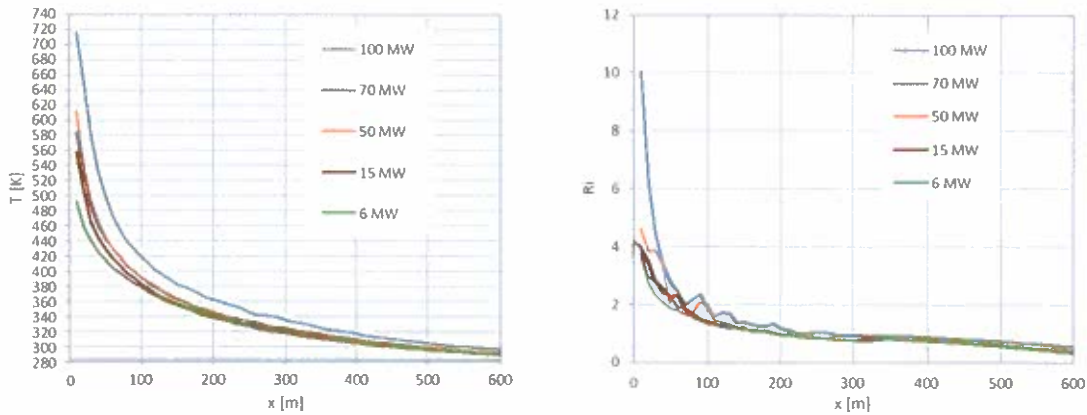


Figure 3 – Temperature and Richardson Number profiles with wind at $t = 30$ min ($v=0.77$)

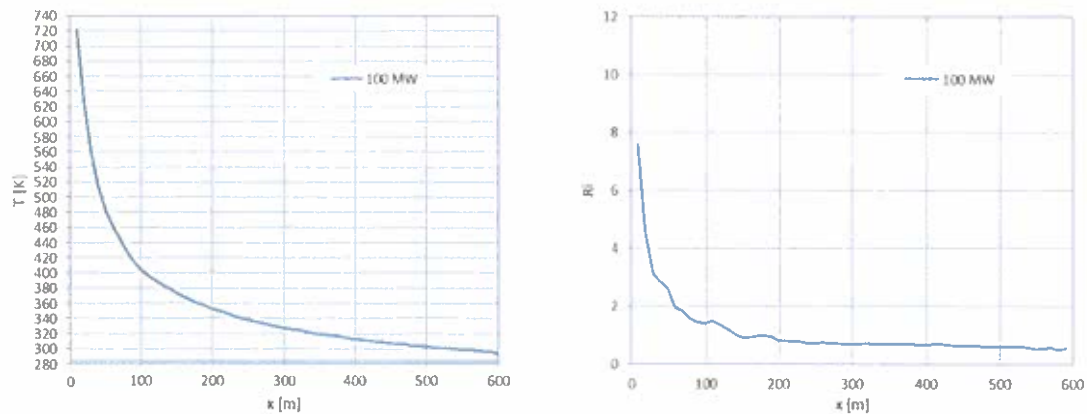


Figure 4 – Temperature and Richardson Number profiles with wind at $t = 30$ min ($v=1.19$ m/s)

Figure 6 presents the contours of soot concentration in the vertical symmetry plane for a horizontal tunnel without wind action and with wind driven velocity of $v = 0,77$ m/s. The red line corresponds to the zero velocity; thus, it represents the boundary between the upper layer outflow and the lower layer inflow. The white lines represent soot concentration of 80 mg/m³ and 300 mg/m³, corresponding to visibility distances for reflecting signs of 5.0 m and 1.3 m, respectively.

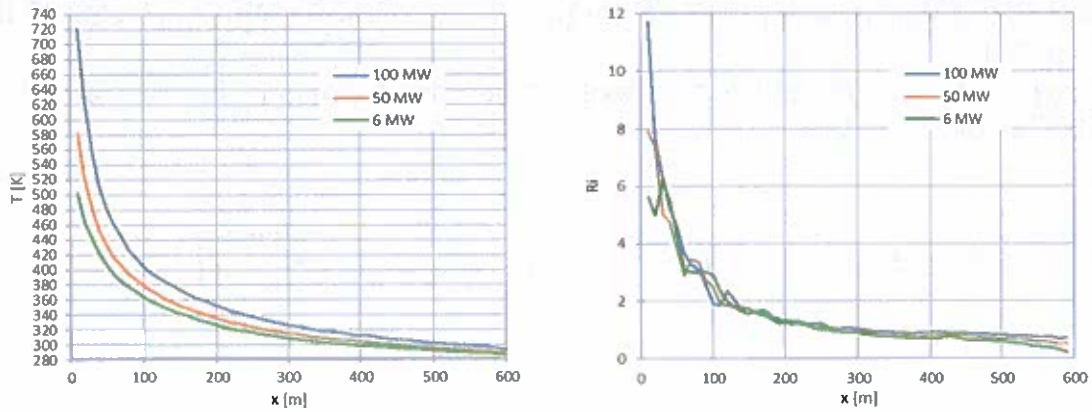


Figure 5 – Temperature and Richardson Number profiles without wind at $t = 30$ min ($v=0$ m/s)

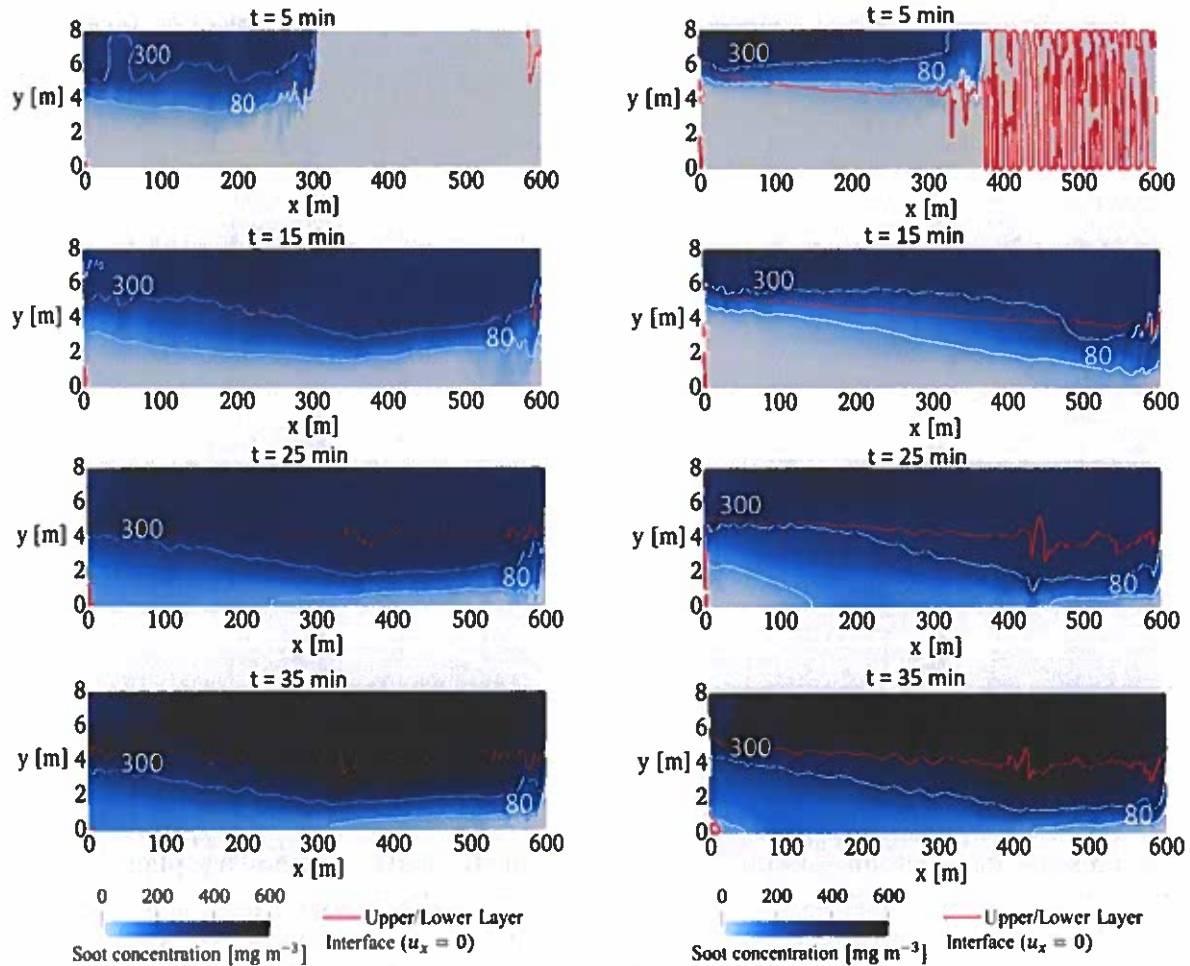


Figure 6 – Comparison of the soot concentration with wind ($v=0.77$ m/s and without wind (right), for a fire with $HRR_{nominal}=50$ MW in a horizontal tunnel

Figure 7 presents the soot concentration in the vertical symmetry plane for a horizontal tunnel with wind velocity of $v = 0.77$ m/s for two different fire source sizes. The development of the smoke contamination is similar but is much more intense for the higher HRR. Moreover, the comparison between Figures 6 and 7 shows that the contamination of the lower inflow layer with smoke increases with the wind velocity v .

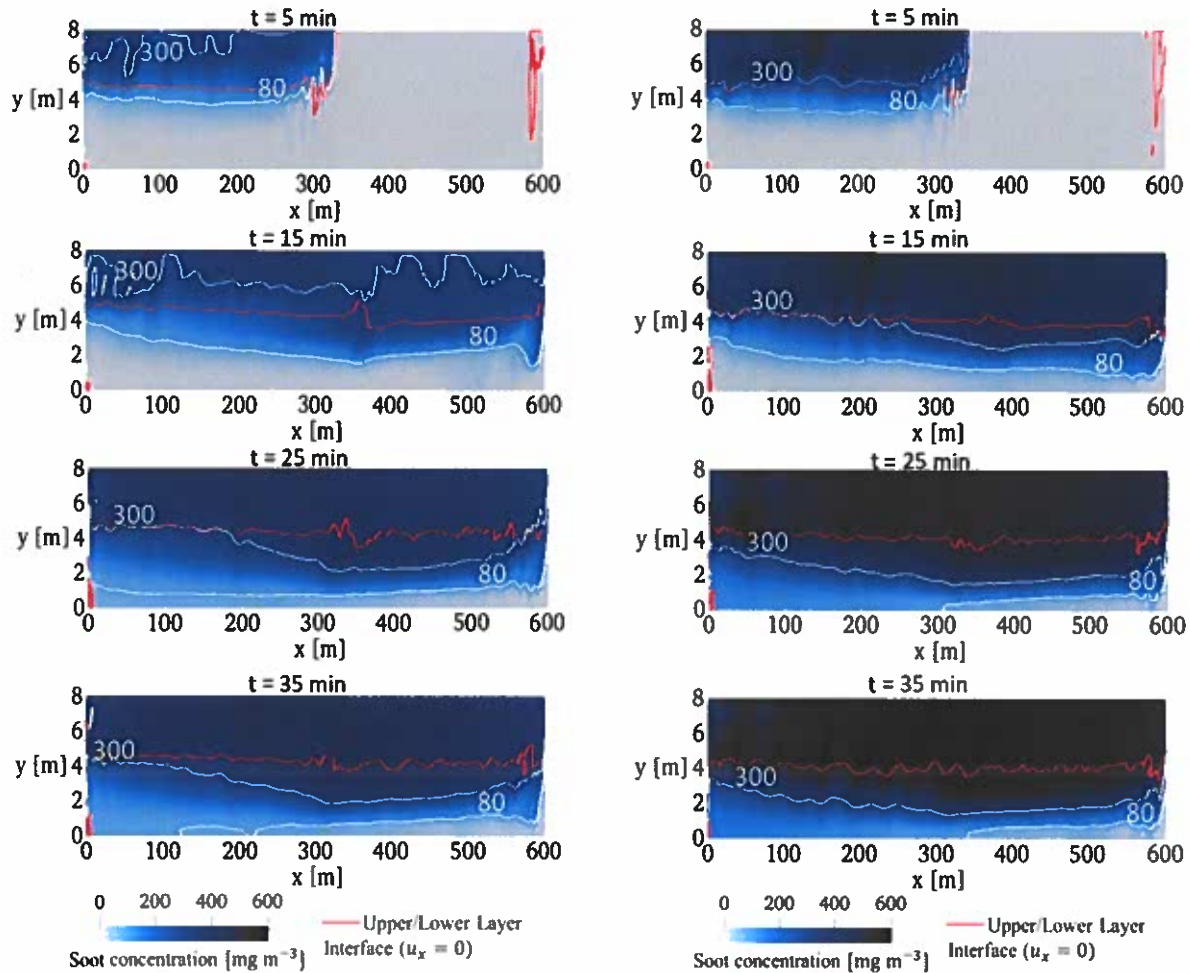


Figure 7 – Comparison of the soot concentration for $HRR_{nominal}=15$ MW (left) and $HRR_{nominal}=70$ MW (right) in a horizontal tunnel and with external wind, $v = 0.77$ m/s

Figures 8 and 9 show the mass flow rate in the upper outflow layer, \dot{m} , and the difference between the velocity magnitudes in the upper and lower layers, Δu , for $v = 0.77$ m/s (with wind) and $v = 0$ m/s (without wind), respectively. When the outflow (higher layer) velocity magnitude is higher ($\Delta u > 0$), the mass entrainment from the lower to the higher layer dominates, thus increasing the upper layer mass flow rate (left side of the figure). However, for $v = 0.77$ m/s, $\Delta u = 0$ occurs at a distance from the fire source smaller than the distance beyond which the decay of the upper layer mass flow rate occurs.

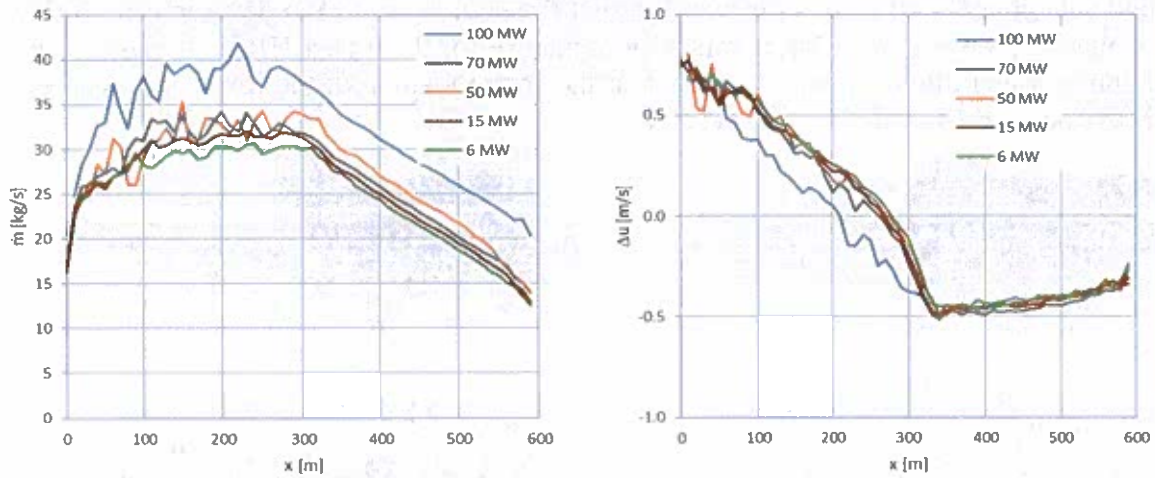


Figure 8 – Mass flow rate in the upper outflow layer, \dot{m} , and difference between velocity magnitudes in the upper and lower layers, Δu , at $t = 30$ min ($v=0.77$ m/s)

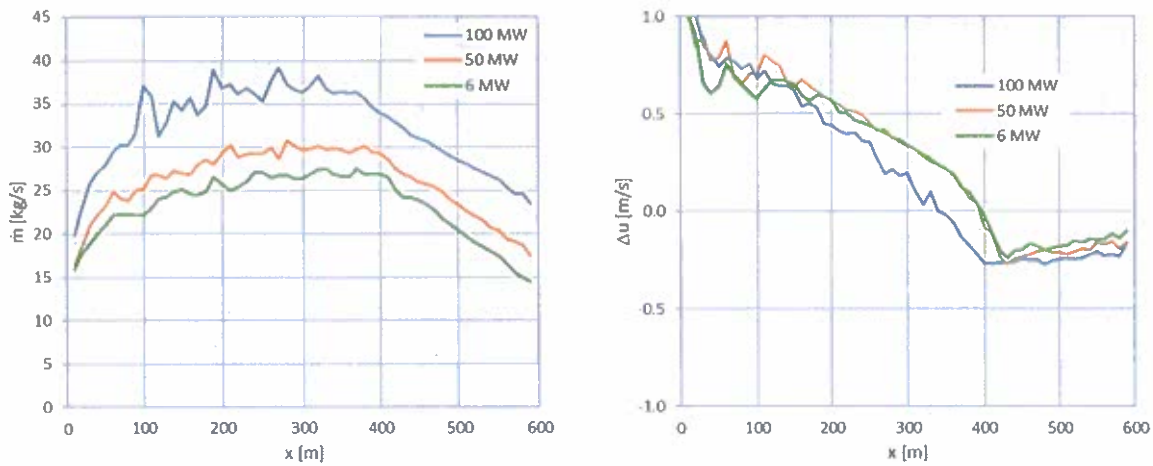


Figure 9 – Mass flow rate in the upper outflow layer, \dot{m} , and difference between velocity magnitudes in the upper and lower layers, Δu , at $t = 30$ min ($v=0$ m/s)

5. DISCUSSION

5.1. General

In this section, several quantities, obtained by CFD simulations, related with the lower layer contamination with smoke during tunnel fires (namely, upper layer mass flow rate, upper layer velocity and lower layer velocity) are analysed. Using the methods proposed by Galhardo et al. [2] and Ortega et al. [3], the results calculated using algebraic equations available in the

literature are compared with the CFD results to clarify the role of the influencing variables. While in the work presented by Galhardo et al. [2] a horizontal tunnel subjected to wind action was studied, Ortega et al. [3] studied the influence of the tunnel slope for the same tunnel and heat release rate. In this work, the same horizontal tunnel is used again, but different heat release rates from the fire source combined with the wind action were considered. This does not constitute a predictive model yet, because several data were taken from the CFD results, but it is intended to be a step towards an algebraic model able to predict the beginning of the lower layer contamination with smoke.

As noticed by Galhardo et al. [2], the shear layer between the upper and lower layer is responsible by the entrainment of air from the lower layer to the upper layer causing the mass transfer that increased the upper layer mass flow rate, while the upper layer absolute velocity is higher than the lower layer absolute velocity. When the upper layer absolute velocity is lower than the lower layer absolute velocity, the mass transfer from the upper layer to the lower layer dominates, and the contamination of the lower layer with smoke starts or is strengthened. Ortega et al. [3] observed that this simple criterium is not possible to apply to slopped tunnels because, due to the stack effect, the mass flow rates in the upper and lower layers are not equal. Consequently, the contamination of the lower layer with smoke starts even when the upper layer absolute velocity is higher than the lower layer absolute velocity. According to Ortega et al. [3], the mass transfer from the upper to the lower layer starts when the lower layer mass flow rate is not able to increase, due to geometric limitation of the tunnel, to satisfy the mass balance. In this section, the equations proposed by Ortega et al. [3] are used and, whenever necessary, they are adapted considering the physical constraints.

5.2. Upper layer velocity

The upper layer velocity in the vicinity of the fire is obtained from equation 4 [3]:

$$\Delta v_u = \frac{S_u \rho_\infty \left(1 - \frac{T_\infty}{T_u}\right) c g - S_u f \rho_\infty \frac{T_\infty v_u^2}{2 T_u D_{H u}} - v_u W \rho_\infty C_\beta (v_u - v_l)}{\dot{M}_u} \Delta x \quad (4)$$

where S_u is the area of the cross-section of the upper layer, ρ_∞ is the density of air at temperature T_∞ , T_∞ is the ambient air temperature, T_u is the average upper layer temperature, c is a proportionality constant, g is the acceleration of gravity, f is the friction factor, v_u is the upper layer average velocity, $D_{H u}$ is the upper layer hydraulic diameter, W is the width of the interface between the upper and lower layers, C_β is a model constant related to the entrainment, v_l is the lower layer average velocity and \dot{M}_u is the upper layer mass flow rate.

On the right side of the equation, the first term is related with the momentum source due to buoyancy, the second one is related with the friction losses in the tunnel walls, ceiling and shear layer (between upper and lower layers) and the third term is related with the momentum losses due to mass transfer from the upper to the lower layer.

The initial velocity (v_u for $x=10$ m), the coefficient c (that affects the term of increment of velocity due to buoyancy) and the friction factor (f) are obtained by the least squares method best fit. The solutions obtained showed that the coefficient $C_\beta = 0$, meaning that the momentum losses due to mass transfer from the upper to the lower layer is much less relevant than the buoyancy and friction losses; therefore, the equation was simplified to equation 5:

$$\Delta v_u = \frac{S_u \rho_{\infty} \left(1 - \frac{T_{\infty}}{T_u}\right) c g - S_u f \rho_{\infty} \frac{T_{\infty} v_u^2}{2 T_u D H u}}{M_u} \Delta x \quad (5)$$

The values obtained are presented in the Table 2 and some selected results are presented in Figure 10, where $v_u(10)$ means the value of v_u for $x=10$ m.

HRR [MW]	100	50	6	100	70	50	15	6	100
Wind [m/s]	0	0	0	0.771	0.771	0.771	0.771	0.771	1.19
$v_u(10)$ [m/s]	1.35	1.09	0.98	1.62	1.40	1.25	1.34	1.21	1.59
c	0.0010	0.0011	0.0011	0.001	0.002	0.002	0.002	0.002	0.0009
f	0.017	0.018	0.017	0.021	0.031	0.031	0.032	0.034	0.021

Table 2. Best fit obtained by the least squares method.

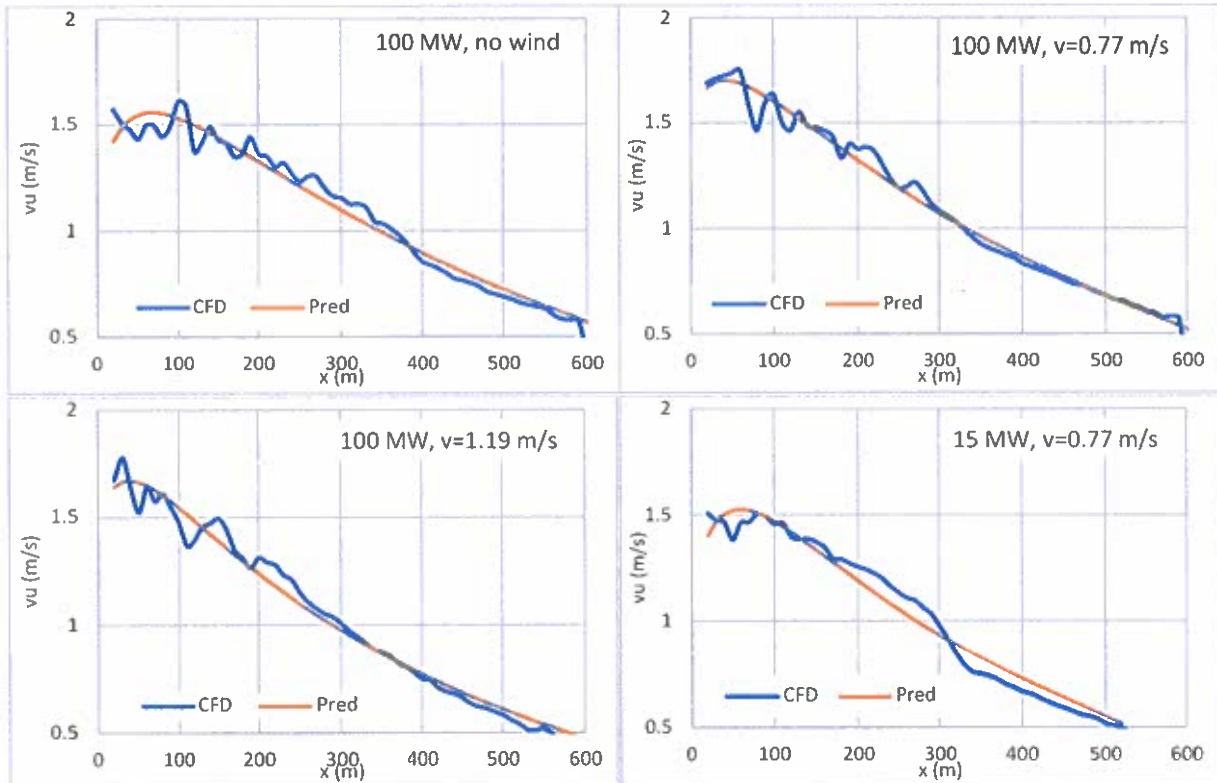


Figure 10. Comparison between the predicted (Pred2) and simulated (CFD) upper layer velocity for 100 MW (without wind, $v=0.771$ m/s and $v=1.19$ m/s) and for 15 MW ($v=0.771$ m/s).

Figure 10 shows that the upper layer velocity slightly increases close to the fire source and decreases farther downstream. The increment of the upper layer velocity as the distance from the fire increases is due to the buoyancy term, where the parameter “ c ” lies in the range of 0.0009 to 0.002. This range is about two orders of magnitude smaller when compared with the values obtained by Ortega *et al.* [3] for sloped tunnels. In our case, the tunnel is horizontal,

therefore the buoyancy effect is weaker because it is just related with the upper hot layer thickness and not with the height difference between tunnel extremities. The decrease of the upper layer velocity at a larger distance from the fire is due to the friction loss term. The friction factor lies in the range of 0.017 to 0.034. Ortega *et al.* [3] reported a range from 0.020 to 0.035, which is very similar. This factor also includes the friction losses in the shear layer between the upper and lower layers, which are not explicitly considered in Equation 5. The value $f = 0.020$ is currently used in tunnels with concrete walls [9]. The f value is higher for the cases under the wind action and increases when the heat release rate is reduced. The wind effect is not explicitly considered in equation 4, then the least squares fit reflects the wind effect on the friction losses term.

The Figure 10 shows that the upper layer velocity increases with the heat release rate of the fire source. The opposing wind effect reduces the upper layer velocity far from the fire source.

5.3. Upper layer mass flow rate

The initial mass flow rate is obtained from the CFD simulation for $x=10$ m. The upper layer mass flow rate variation is obtained from equation 6 [3]:

$$\Delta \dot{M}_u = \rho_\infty W C_\beta (v_u - v_l) \Delta x \quad (6)$$

where $C_\beta = 0.004$ is a model constant related to the entrainment coefficient β .

Figure 11 shows the prediction of the upper layer mass flow rate using equation 6. Is clear that, far from the fire source, the entrainment process is weaker, and it is not possible to express it by equation 6. Beyond some distance from the fire source, the upper layer mass flow rate decreases, meaning that the upper layer starts losing mass to the lower layer and contaminates the lower layer with smoke.

5.4. Lower layer velocity

The lower layer velocity is obtained from equation 7 [3]:

$$v_l^* = \frac{\dot{M}_u}{\rho_\infty (S - S_u)} \quad (7)$$

where S is the tunnel cross section area. This equation expresses the mass balance between the upper and the lower layer without wind and for a horizontal tunnel.

The lower layer velocity is modified by the wind effect (the wind increments the lower layer velocity). The lower layer velocity v_l was predicted by treating the flow as a superposition of a tunnel fire without wind (in which case v_l^* can be calculated by equation 7) and a wind flow without a fire (with the average velocity v inside the tunnel), according to equation 8 [2].

$$v_l = \sqrt{v_l^{*2} - v^2} \quad (8)$$

Figure (12) compares the lower layer average velocity obtained by CFD and by equations (7) and (8). As the prediction of the lower layer average velocity depends on the upper layer mass flow rate prediction, the lower layer velocity increases with x to satisfy mass balance when the upper layer mass flow rate increases (the lower layer is at ambient air temperature). Far from the fire source, the lower layer velocity predicted by Equation 8 diverges from the CFD results due to the process of mass transfer from the upper to the lower layer.

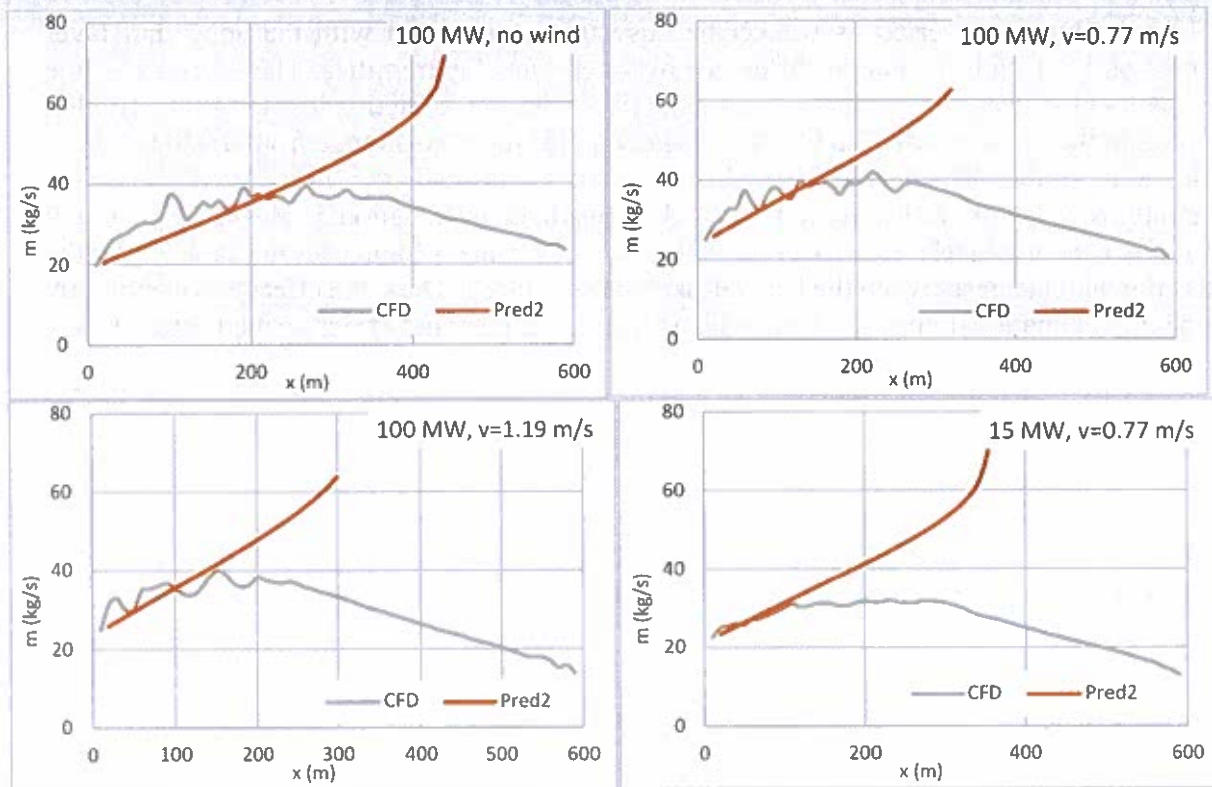


Figure 11. Comparison between the predicted (Pred2) and simulated (CFD) upper layer mass flow rate for 100 MW (without wind, $v=0.771$ m/s and $v=1.19$ m/s) and for 15 MW ($v=0.771$ m/s).

5.5. Origin of the lower layer contamination

equations (5) and (7) may be used to determine when it is physically unrealistic to consider the upper- and lower-layer flows without significant mixing. These flows are driven by the buoyancy. The maximum difference between the upper layer and lower layer velocities of the flow due to buoyancy may be predicted by the equation 9 [3]:

$$\Delta v = \sqrt{2g \left(\frac{T_u}{T_\infty} - 1 \right) h_u} \quad (9)$$

The prediction of the distance x_c from the fire source where the contamination of the lower layer with smoke starts is based on the comparison between the difference of the predicted upper and lower layer velocities (using equations (5) and (7)) with the maximum difference between the upper layer and lower layer velocities of the flow due to buoyancy (equation (9)). Figure 13 shows the lines corresponding to the predicted difference between the upper layer and lower layer velocities (u_{dif_pred}), which is obtained using Equations (5) and (7), and the maximum allowed velocity difference due to the temperature inside the tunnel (u_{dif_max}), which is given by equation (9).

The blue arrows indicate the intersection of the lines u_{dif_pred} and u_{dif_max} . For large

distance from the fire source, namely beyond this intersection, it is not possible to increase the velocity difference between both layers because the buoyancy action is insufficient; therefore, the only physical solution is to transfer mass from the upper layer to the lower layer. The red arrows indicate the points where the upper layer mass flow rate starts to decrease significantly according to the CFD predictions. These points correspond to the beginning of a significant contamination with smoke of the lower layer. Table 3 compares the values of the distance x_c obtained by CFD and by the predictions from equations (5) and (7).

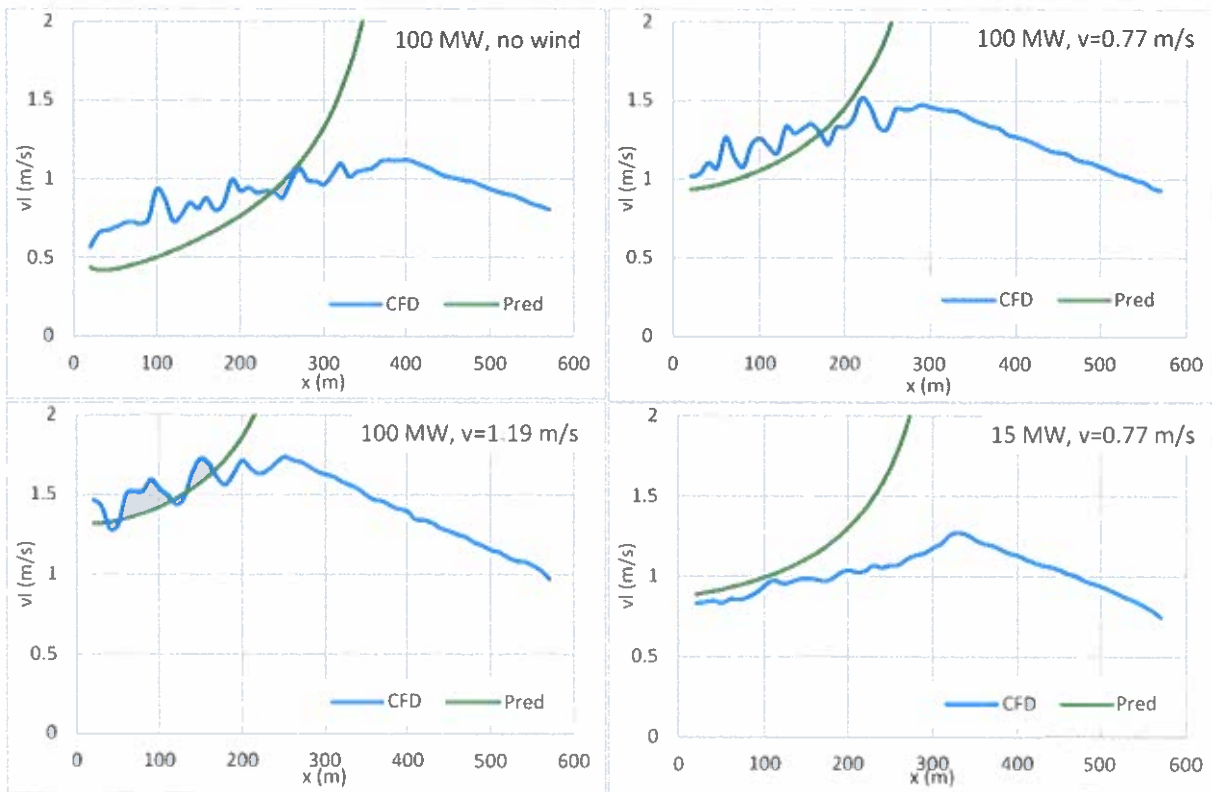


Figure 12. Comparison between the predicted (Pred2) and simulated (CFD) lower layer velocities for 100 MW (without wind, $v=0.771$ m/s and $v=1.19$ m/s) and for 15 MW ($v=0.771$ m/s).

Table 3 shows that the values of the distance x_c obtained by CFD and by the predictions from equations (5) and (7) are quite close. The relative error of the prediction based on the algebraic equations, and taking the CFD results as reference, is higher for the lower heat release rate and for the condition without wind. The predicted x_c value is always smaller than that obtained by the CFD simulations, thus it is in the safe side. The value of x_c obtained for $Ri=0.8$ is a general criterium that is used to assess the possibility of loss of thermal stratification when the difference of temperature between the hot and cold layers is too small and the opposing velocities of both layers too high [10, 11]. Observing the difference between the values of x_c determined from the CFD results and the values obtained for $Ri=0.8$, this criterium is not applicable in tunnel fire scenarios, where the flow is constrained.

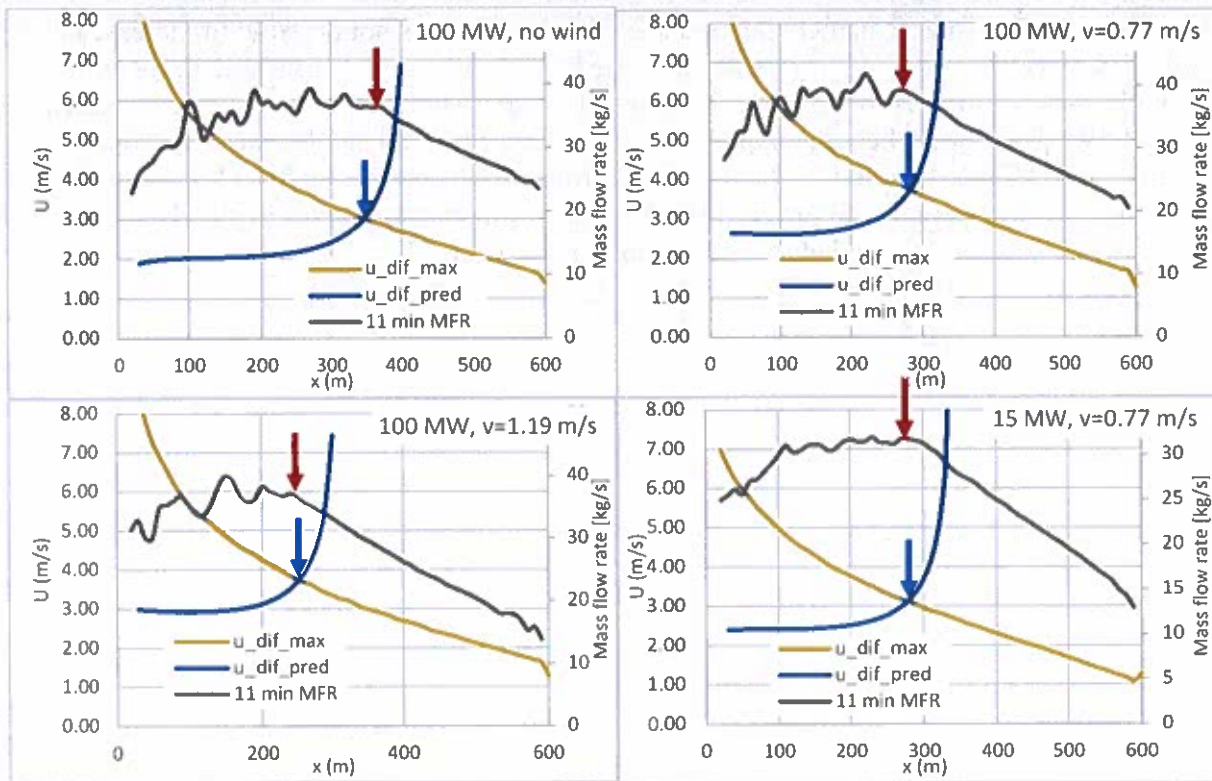


Figure 13. Comparison between the predicted difference between the upper layer and lower layer velocities (u_dif_pred) and the maximum allowed velocity difference for 100 MW (without wind, $v=0.771$ m/s and $v=1.19$ m/s) and for 15 MW ($v=0.771$ m/s).

HRR [MW]	100	50	6	100	70	50	15	6	100
Wind v [m/s]	0	0	0	0.771	0.771	0.771	0.771	0.771	1.19
CFD x_c [m]	380	380	380	270	270	290	270	310	250
x_c for $Ri=0.8$ [m]	520	450	320	450	370	370	350	260	220
Predicted x_c [m]	350	360	350	280	270	280	270	270	250
Error [%]	8	5	8	4	0	3	0	13	0

Table 3. Longitudinal coordinate x_c corresponding to the beginning of the lower layer smoke contamination: comparison between simulated (CFD) and predicted values.

The distance x_c decreases when the opposing wind velocity increases, as concluded by Ortega et al. [3], but seems insensitive to the variation of the heat release rate. When the heat release rate increases, the velocity increases; this seems to be the reason why the distance x_c is not significantly affected by the heat release rate variation.

6. CONCLUSIONS

Large eddy simulations of naturally ventilated tunnel fires were performed with fireFoam to study the effect of the variation of the heat release rate (HRR) both with and without wind in a naturally ventilated tunnel. Experimental data available in the literature for the Memorial Tunnel was used for validation purposes. It shows that, although the velocity due to buoyancy increases with the HRR, the location of the lower layer contamination with smoke does not vary significantly. It is concluded that the criterium based on the Richardson Number ($Ri=0.8$), commonly used to assess the possibility of thermal stratification loss, is not applicable when the flow is constrained in tunnel fire scenarios.

It is also shown that the criterium based on the higher and the lower layer velocities and the balance of the mass flow rates of the layers, formerly proposed by Ortega *et al.* [3], may correctly predict the distance from the fire source where the lower layer contamination with smoke starts.

REFERENCES

- [1] Directive 2004/54/EC of the European Parliament and of the Council of 29 April 2004, on minimum safety requirements for tunnels in the Trans-European Road Network.
- [2] A. Galhardo, J. Viegas and P. Coelho. *The influence of wind on smoke propagation to the lower layer in naturally ventilated tunnels*. Tunn. Undergr. Space Technol. 2022, 128, 104632.
- [3] E. Ortega, J.C. Viegas and P.J. Coelho. *The contamination of the lower layer in sloped tunnel fires*. Fire, 2023, 6, 245.
- [4] A. Galhardo, J. Viegas, P. Coelho, E. Ortega and U. Fernandes. *Smoke control in naturally ventilated tunnels*. 2nd International Conference on Road Tunnel Operations and Safety. Granada (Spain), 25th - 28th October 2022.
- [5] H. Guo, Z. Yang, P. Zhang, Y. Gao, Y. Zhang. *Experimental Investigation on Fire Smoke Temperature under Forced Ventilation Conditions in a Bifurcated Tunnel with Fires Situated in a Branch Tunnel*. Fire 2023, 6, 473. <https://doi.org/10.3390/fire6120473>.
- [6] Bechtel/Parsons Brinckerhoff, 1995. *Memorial Tunnel Fire Ventilation Test Program*. Test Report. Massachusetts Highway Department.
- [7] C. Caliendo, G. Genovese, I. Russo. *Risk analysis of road tunnels: A computational fluid dynamic model for assessing the effects of natural ventilation*. Applied Sciences, 11(1):32, 2021.
- [8] J. Kong, W. You, Z. Xu, H. Liu, H. Li. *A Numerical Study on Smoke Behaviors in Inclined Tunnel Fires under Natural Ventilation*. Journal of Safety Science and Resilience (2022).
- [9] Centre d'Etudes des Tunnels. *Dossier Pilote des Tunnels Équipements*; Centre d'Etudes des Tunnels: Bron, France, 2003.
- [10] P. L. Hinkley. *The flow of hot gases along an enclosed shopping mal. A tentative theory*. 1970.
- [11] D. Yang, L.H. Hu, R. Huo, Y.Q. Jiang, S. Liu, F. Tang. *Experimental study on buoyant*

flow stratification induced by a fire in a horizontal channel. Applied Thermal Engineering 30 (2010) 872–878.